Experimental Study of Hot Deformability Of 1.2690 Tool Steel - Preeliminary Results

Experimentalna študija tople preoblikovalnosti 1.2690 orodnega jekla - preliminarni rezultati

T. Večko Pirtovšek[1], G. Kugler[1], M. Godec[2], R.Turk[1] and M. Terčelj[1]

[1] Faculty of Natural Sciences and Engineering University of Ljubljana, Ljubljana, Slovenia
[2] Institute of Metals and Technology, Ljubljana, Slovenia;
E-mail: milan.tercelj@ntf.uni-lj.si

Received: June 15, 2006 **Accepted**: July 20, 2006

Abstract: 1.2690 is a high alloyed cold work tool steel with about 1.1 % C, 0.3 % Si, 0.3 % Mn, 11 % Cr, 1.5 % V, 2.3 % W and 1.3 % Mo. As such it has a lot of ledeburitic carbides in microstructure, thus its hot plasticity should be investigated. For this purpose hot compression tests of cylindrical specimens, taken from annealed forged billet square 95 mm, were carried out on thermo-mechanical simulator Gleeble 1500D in order to establish suitable parameters for hot working of mentioned tool steel. The temperature range was 850 °C to 1200 °C and the strain rates varied from 0.001 s^{-1} to 6 s^{-1}. Special attention was paid to mechanisms, which are responsible for poor plasticity at upper and lower border of temperature range of hot working. Hot deformation behaviours of steel CRV3 have been studied also by using Prasad's processing (efficiency of power dissipation) and instability maps developed on the basis of dynamic materials model. 1.2690 tool steel exhibits flow instability at lower strain rates and temperatures.

Povzetek: 1.2690 je visokolegirano orodno jeklo za delo v hladnem s približno 1,1 % C, 0,3 % Si, 0,3 % Mn, 11 % Cr, 1,5 % V, 2,3 % W and 1,3 % Mo. V mikrostrukturi je prisotno veliko ledeburitnih carbidov kar zmanjšuje njegove toplo plastičnost. Za njeno raziskavo smo na Gleeble 1500D termomehanskem simulatorju izvedli tople stiskalne preizkuse s cilindričnimi vzorci izrezanih iz kvadratne gredice (95 mm x 95 mm). Na ta način smo dobli primerne parametre za toplo preoblikovanje omenjenega jekla. Testi so bili izvedeni v temperaturnem območju 850 °C to 1200 °C in hitrostih deformacije v območju 0,001 s^{-1} to 6 s^{-1}. Posebna pozornost je bila namenjena mehanizmom, ki so odgovorni za slabo plastičnost na zgornji in spodnji meji varnega toplega preoblikovanja. Toplo stiskanje je bilo študirano tudi s pomočjo Prasadovih procesnih map ter mapami nestabilnosti. Te nam razkrijejo nestabilna področja preoblikovanja pri nižjih teperaturah in nižjih hitrostih deformacije.

Keywords: 1.2690 tool steel; hot compression; flow curves; processing maps
Ključne besede: 1,2690 orodno jeklo; toplo stiskanje; krivulje tečenja; procesne mape

Scientific paper

INTRODUCTION

High alloyed tool steels cause a lot of production problems due to their narrow hot working temperature range and low hot ductility and as such they usually belong to a low deformable steel. Due to the already mentioned problems, the economy of production and quality of products should be further improved also by means of a better knowledge of behavior (processes) of steel during its hot forming. There is little work published in scientific literature on hot workability of tool steel; thus, more contribution from this research area is desired [1-4]. Ledeburitic cold work tool steel CRV3 (1.2690) contains many alloying elements and ledeburitic carbides. It results in a high strength and hardness, small deformation during heat treatment, very good wear resistance, and also in poor ductility (plasticity) during its hot deformation. Its microstructure during hot deformation can be characterized as a two-phase system consisting of austenite matrix and a combination of ledeburitic carbides. The total volume fraction of carbides is in the range of about 9 - 19 %, depending on heat treatment condition [5]. The distribution, the quantity and size of carbides in ledeburitic tool steel have a large effect on its hot deformation behavior. Both the dissolution of alloying elements and the precipitation of carbides result in strengthening the tool steel during hot deformation. In order to prevent hot cracking and microstructural damage during the several deformation steps of a hot working process it is necessary to understand the interaction between the strain hardening and softening mechanisms governing the flow behavior of the matrix compound between the primary carbides.

The objective of this work is to investigate hot workability of 1.2690 tool steel, i.e. to find the optimum working conditions, to find out the upper and lower limits of parameters of hot working and to study the reasons of hot cracking. Prasad's processing map was used to reveal the instable zone of working conditions.

EXPERIMENTAL TECHNIQUES

The chemical composition of CRV 3 tool steel is given in Table 1. The cylindrical specimen dimensions ϕ 10 mm x 15 mm were machined from an annealed forged billet square 95 mm. Center lines of specimens were orthogonal to longitudinal direction of the billet. Because of some microstructural inhomogeneity across the section of a forged billet, all the compression specimens were taken from the same depth of a square billet. The initial microstructure of applied samples is given in Figure 1.

Physical simulation of hot forming process was carried out on Gleeble 1500D thermo-mechanical simulator. The following testing conditions were chosen: the temperature range 850 °C to 1200 °C, strain rates of 0.001 s^{-1} - 6 s^{-1} and true strains of 0 - 0.9 (Table 2). The tantalum follies thickness of 0.05 mm were inserted between cylindrical specimen and compression tool (anvil) to avoid inhomogeneous deformation. The nominal maximum strain for all tests was cca 0.9. After deformation, specimens were water quenched to freeze over their microstructure. The following parameters were measured during tests: compression force, temperature of cylindrical specimen, shift of active jaws (sample height). The

Table 1: Chemical composition of the 1.2690 steel in wt. %

	C	Si	Mn	Cr	V	W	Mo
1.2690	1.17	0.24	0.26	11.3	1.48	2.24	1.35

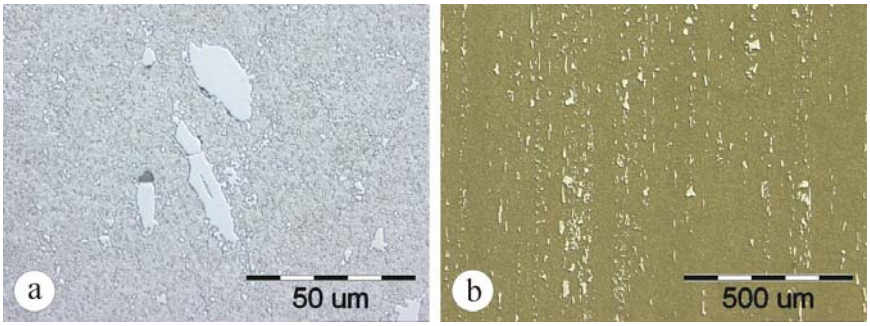

Figure 1: The initial microstructure of a forged billet square 95 mm:
(a) quenched microstructure, (b) distribution of carbides

Table 2: Deformation conditions

Deformation temperature / ºC	Strain rate / s^{-1}
850, 900, 950, 1000, 1050, 1100, 1150, 1160, 1170, 1180, 1200	0.001, 0.01, 0.1, 1.0, 6.0

strain rate was programmed as a constant value. These data were the basis for calculating of the stresses and strains and for the evaluation of flow curves. The temperature of deformed samples was measured continuously with a thermocouple during the deformation, so that the deformation heating could be corrected.

Deformed samples were visually surveyed and then longitudinally cut for the preparation of matallographic samples.

Results

True stress-strain (σ–ε) curves

The typical stress-strain curves in the range of 850 °C to 1200 °C and strain rates of 0. 01 s^{-1} and 1 s^{-1} are shown in Figure 2. All flow curves at all strain rates exhibit a maximum, which is a result of dynamic softening - dynamic recovery and dynamic recrystallisation. The maximum is very clear at low temperatures, 850 - 900 °C. Lower testing temperature and lower strain rates result in more emphasized peaks and vice versa. It can be seen that the strain corresponding to the peak flow stress increases with the decrease in temperature and with the increment of strain rate. However, decreasing temperature and increasing strain rate will delay the onset of dynamic softening. The peak of flow stress is in the strain range of 0.05 - 0.3.

In order to present more clearly the relationship between deformation temperature, strain rate and maximal stress, the peak stresses are

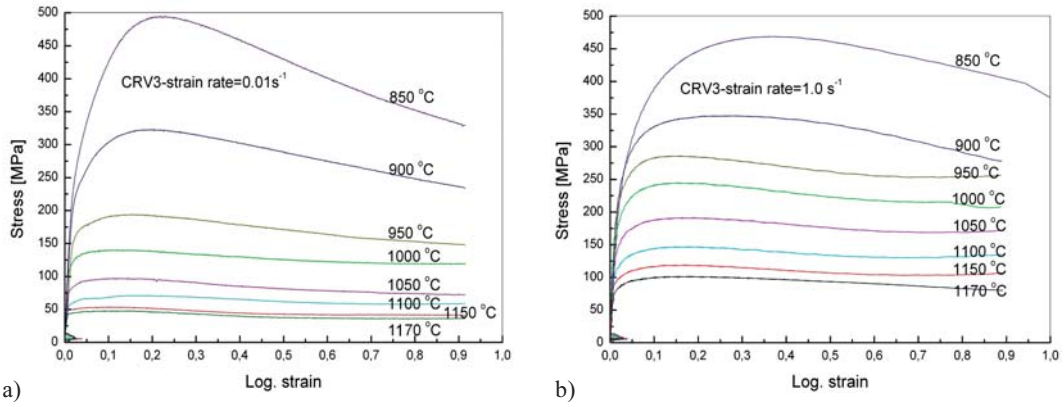

Figure 2: Stress-strain curves in the range of 850 °C to 1170 °C: (a) strain rate 0.01 s-1, (b) strain rate 1.0 s^{-1}

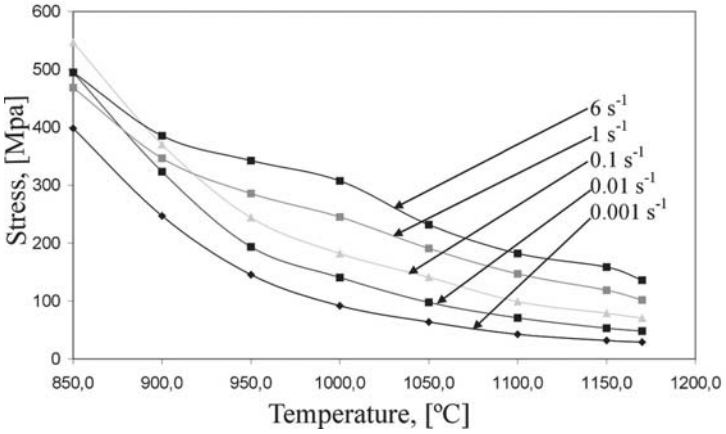

Figure 3: Dependence of the peak of flow stress on temperature for different strain rates (0.001 s^{-1} - 6 s^{-1})

plotted against the temperature for different strain rates in Figure 3. With decreasing of temperature in the temperature range 1170 - 1000 °C and with increasing of strain rate the peaks of flow stress also increase almost proportionally. This behaviour changes at temperature 1000 °C; namely the increase of peak of flow stress of strain rates 0.001 s^{-1} - 0.1 s^{-1} is much higher in comparison to strain rates 1 s^{-1} - 6 s^{-1}. Thus at 900 °C the peak value of strain rate of 0.1 s-1 exceeds the peak value of strain rate 1 s-1 and at 850 °C also the peak value of 6 s^{-1}.

Influence of test parameters on macro cracks

The sample deformed at 1200 °C and presented on Figure 4a is completely destroyed, while the sample deformed at 1180 °C shows a lot of macroscopic surface cracks occurring parallel to the direction of compression axis (Figure 4b). The samples deformed at temperatures 1160 °C, 1100 °C, 1050 °C, 1000 °C, 950 °C, 900 °C and 850 °C do not exhibit any cracks (Figure 4c), except a sample deformed at 850 °C and

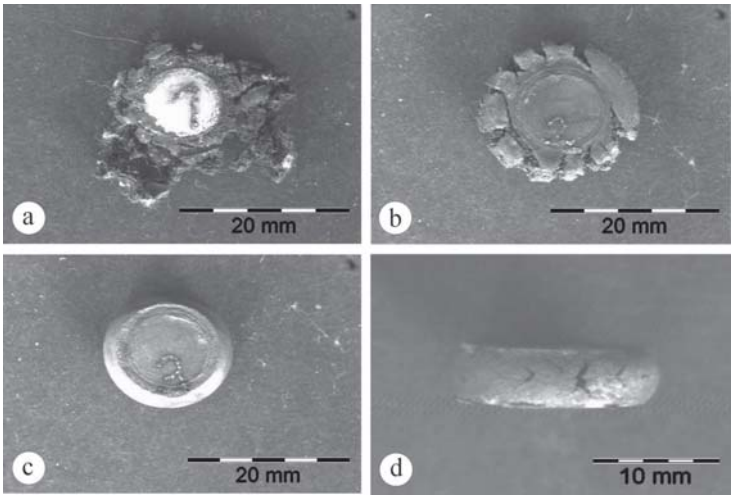

Figure 4: Macrograph of deformed samples (a) 1200 °C, strain rate 6 s^{-1}, (b) 1180 °C, strain rate 6 s^{-1} , (c) 1160 °C, strain rate 6 s^{-1}, (d) 850 °C, strain rate 0.01 s^{-1}

strain rate 0.01 s^{-1} (Figure 4d). This sample exhibits typical surface cracks occurring parallel to the direction of the main stress.

Influence of test parameters on microstructure

The microstructure of deformed and water quenched samples is austenitic with different contents of martensite and carbides. Figure 5 represents microstructures of some samples deformed at strain rates 6 s^{-1} and 0.01 s^{-1}. On deformation temperatures between 1160 °C and 1200 °C the ledeburitic carbides dissolve to a great extent (Figures 5a-b). During the deformation at temperature 1160 °C, a precipitation of a thin layer of carbides along grain boundaries occurs (Figures 5b-c), and at higher temperatures, a new eutectic appears (Figure 5a). Melting on grain boundaries causes the weakening of grain boundaries and cracking of steel. At lower deformation temperatures to about 1100 °C and at strain rate 6 s^{-1}, the microstructure is recrystallised, composed of equiaxial grains (Figure 5d). At deformation temperature 1050 °C, the crystal grains are also equiaxial, but they are arranged within the earlier deformed austenitic crystal grains (Figure 5e). The majority of carbides is arranged along the earlier deformed austenitic crystal grains. For deformation temperatures 1000 °C and lower, deformed initial austenitic crystal grains and carbide precipitation along them are typical (Figure 5f). The grain boundaries were not revealed by etching very well. At the strain rate 0.01 s^{-1}, recrystallisation is running completely at temperature 1150 °C only (Figure 5g), while at temperature 1050 °C deformed initial austenitic crystal grains with some equiaxial crystal grains within predominate (Figure 5h).

During the cooling from the austenitization temperature and under 1000 °C the precipitation of secondary carbides along austenite grain boundaries takes place. With decreasing temperature the mentioned precipitation process accelerates that causes an intensive weakening of primary grain boundaries. At temperature 1000 °C the

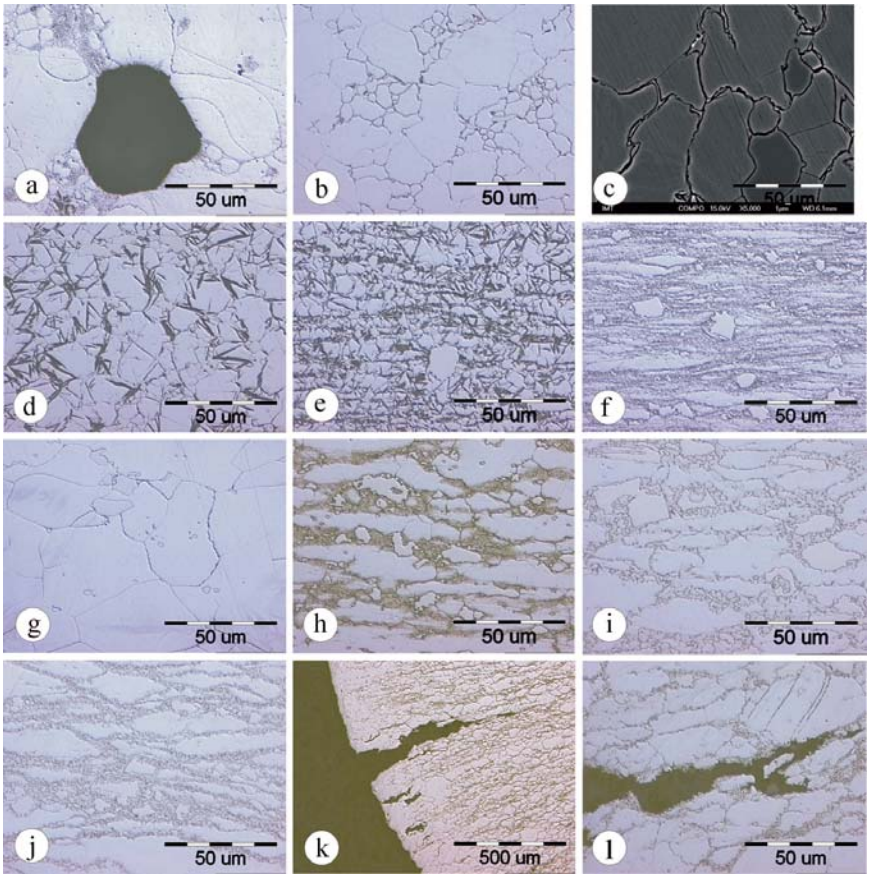

Figure 5: Microstructures of deformed samples: (a) 1200 °C, 6 s^{-1}, (b) 1160 °C, 6 s^{-1}, (c) 1160 °C, 6 s^{-1}, (d) 1100 °C, 6 s^{-1}, (e) 1050 °C, 6 s^{-1}, (f) 850 °C, 6 s^{-1}, (g) 1150 °C, 0.01 s^{-1}, (h) 1050 °C, 0.01 s^{-1}, (i) 950 °C, 0.01 s^{-1}, (j, k, l) 850 °C, 0.01 s^{-1}

precipitation of secondary carbides starts along the deformed initial austenitic crystal grains, which are getting clearer along with the deformation temperature lowering (Figure 5i); at temperature 850 °C, it causes an intensive weakening of crystal boundaries resulting in intercrystalline cracks (Figures 5j-l).

PROCESSING MAP

Processing map is developed on the basis of a dynamic material model (DMM) which has been developed and widely used by the group of Y. V. R. K. PRASAD[6, 7]. The processing map of material can be described as an explicit representation of its response to the imposed process parameters. It is a superimposition of the efficiency of power dissipation and an instability map.

Efficiency of power dissipation

The workpiece under hot deformation conditions of this model works as an essential energy dissipater. The constituent equation describes the manner in which energy (P) is converted at any instant into two forms, thermal energy (G) making temperature increase and microstructural change caused by transform of metallurgical dynamics (J), which are not recoverable. In general, most of the dissipation is due to a temperature rise and only a small amount of energy dissipates through microstructural changes. The power partitioning between G and J is controlled by the constitutive flow behavior of the material and is decided by the strain rate sensitivity (m) of flow stress as shown in the Equation

$$\frac{dJ}{dG} = \frac{\dot{\bar{\varepsilon}}\, d\bar{\sigma}}{\bar{\sigma}\, d\dot{\bar{\varepsilon}}} = \frac{\dot{\bar{\varepsilon}}\,\bar{\sigma}\, d\ln\bar{\sigma}}{\bar{\sigma}\,\dot{\bar{\varepsilon}}\, d\ln\dot{\bar{\varepsilon}}} \approx \frac{\Delta\log\bar{\sigma}}{\Delta\log\dot{\bar{\varepsilon}}} = m \qquad (1)$$

For an ideal dissipator it can be shown that both quantities J and G are equal in their amount, which means that $m = 1$ and $J = J_{max}$ whereas the efficiency of power dissipation η is given by:

$$\eta = \frac{J}{J_{\max}} = \frac{2m}{m+1} \qquad (2)$$

The variation of η with temperature and $\dot{\varepsilon}$ represents the relative value of energy dissipation occurring through microstructural changes. Microstructural changes can be stable, which includes a dynamic recovery and dynamic recrystallization, and instable which includes wedge cracking, void formation at hard particles, dynamic strain ageing and macrostructural cracking. As new surfaces will form during instable changes, more energy is required, while stable changes always take place by grain boundary migration.

Flow instability

The instability map is defined by a stability criterion for a dynamic material, where the differential quotient of its dissipative function has to satisfy an inequality condition, given by Equation 10, to allow a stable flow.

$$\xi\left(\dot{\bar{\varepsilon}}\right) = \frac{\partial \ln(m/(m+1))}{\partial \ln\dot{\bar{\varepsilon}}} + m > 0 \qquad (3)$$

Figures 6a-b represents processing and instability contour map for temperature range from 850 °C to 1160 °C and strain rates 0.001 s^{-1} to 6 s^{-1} at strains 0.2 and 0.6. The maps are relatively similar at various strains, but at all strains the instable zone with $\xi < 0$ appears in the temperature range between 850 °C and 970 °C at strain rates about 0.1 s^{-1} - 0.01 s^{-1}. This also proves the Figure 4d and Figures 5k-l (brittle cracking on grain boundary due to precipitation of secondary phases). At lower strains the instable zone moves towards lower strain rates and temperatures and at higher strains towards higher strain rates and higher temperatures.

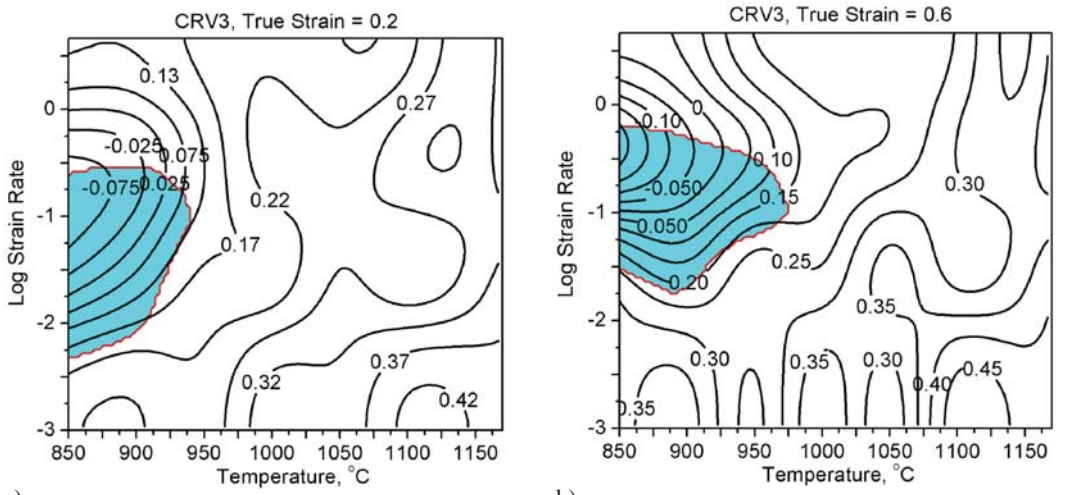

a) b)

Figure 6: Superimposition of power dissipation map and instability map for temperature range from 850 °C to 1160 °C, strain rates 0.001 s^{-1} to 6.0 s^{-1} and at strains 0.2 (a) and 0.6 (b).

DISCUSSION

The optimal deformation conditions for steel 1.2690 are at temperatures between 1000 °C and 1150 °C at strain rates 1.0 - 6.0 s^{-1}. Deformation at higher temperatures may cause incipient melting at grain boundaries and a dramatical drop of hot ductility. The result of deformation at temperatures between 1160 and 1100 °C is a recrystallized microstructure. At lower deformation temperatures, recrystallization is not completed.

During the cooling from the austenitization temperature and under 1000 °C the precipitation of secondary carbides along austenite grain boundaries takes place. Especially this process took place at lower strain rates that resulted in higher peaks stress of flow curves.

Lower strain rates and lower deformation temperatures result in an accelerated precipitation of secondary carbides on grain boundaries and consequently, in increased flow curves. Thus at lower temperature and strain rates higher flow stresses than those at higher strain rates were obtained.

The precipitation of secondary carbides causes also a weakness of grain boundaries and cracking along them. Processing maps ware made for temperature range from 850 °C to 1160 °C and for strain rates between 0.001 s^{-1} and 6.0 s^{-1}. The high temperature region with appearance of incipient melting at grain boundaries was not included in a processing and instability maps. Processing maps at strains 0.2, 0.4 and 0.6 show the some result as the investigation of microstructures of deformed samples. The instable zone appears at strain rates 0.1 s^{-1} - 0.01 s^{-1} and deformation temperatures between 850 and 970 °C, where an intensive precipitation of secondary carbides at grain boundaries occurs.

Conclusion

The optimum deformation conditions for steel 1.2690 are at temperatures between 1000 °C and 1150 °C at strain rates 1.0 - 6.0 s^{-1}. Deformation at higher temperatures may cause incipient melting at grain boundaries and a dramatical drop of hot ductility. During deformation at temperatures below 1000 °C and lower strain rate an intensive precipitation of secondary carbides at grain boundaries occurs and causes a strong work hardening and weakness of grain boundaries. The formerly mentioned secondary precipitation also results in a higher flow stress at lower strain rates in comparison to flow stress at higher strain rates. The experimental results also confirm the predictions of processing maps about the position of the instable zone.

References

[1] C. A. C. Imbert, G. J. McQueen, Hot Ductility of tool Steels, Canadian Metallurgical Quarterly, 40/2 (2001) 235 – 244.

[2] Gao Shan, Liu Xianghua, Wang Guodong, Study on Hot Deformation Cracks of Steel D2 Using Processing Map, J. Iron & Steel Res., Int., 4/2 (1997) 44 - 49.

[3] C. Rodenburg, M. Krzyzanowski, J. H. Beynon, W. M. Rainforth, Hot workability of spray-formed AISI M3:2 high-speed steel, Materials Science and Engineering A, 386 (2004) 420 - 427.

[4] C. Imbert, N. D. Ryan, H. J. McQueen, Hot Workability of Three Grades of Tool Steel, Metallurgical Transactions A, 15A (1984) 1855 - 1864.

[5] Catalogue of Steel Properties of Metal Ravne Company.

[6] Y. V. R. K. Prasad, S. Sasidhara, Hot Working Guide, Compendium of Processing Maps, ASM - International, pp. 1 - 24, OH, USA, 1997.

[7] S. V. S. Narayana Murty, B. Nageswara Rao, B. P. Kashyap, Instability criteria for hot deformation of materials, International Materials Reviews, 45/1(2000) 15 - 26.